International Journal of Engineering, Mathematical and Physical Sciences
ISSN: 2517-9934
Vol:11, No:4, 2017

Conjugate Mixed Convection Heat Transfer and Entropy Generation of Cu-Water Nanofluid in an Enclosure with Thick Wavy Bottom Wall

Sanjib Kr Pal, S. Bhattacharyya

***Abstract*—**Mixed convection of Cu-water nanofluid in an enclosure with thick wavy bottom wall has been investigated numerically. A co-ordinate transformation method is used to transform the computational domain into an orthogonal co-ordinate system. The governing equations in the computational domain are solved through a pressure correction based iterative algorithm. The fluid flow and heat transfer characteristics are analyzed for a wide range of Richardson number $(0.1 \leq Ri \leq 5)$, nanoparticle volume concentration $(0.0 \leq \varphi \leq 0.2)$, amplitude $(0.0 \leq \alpha \leq 0.1)$ of the wavy thick- bottom wall and the wave number (ω) at a fixed Reynolds number. Obtained results showed that heat transfer rate increases remarkably by adding the nanoparticles. Heat transfer rate is dependent on the wavy wall amplitude and wave number and decreases with increasing Richardson number for fixed amplitude and wave number. The Bejan number and the entropy generation are determined to analyze the thermodynamic optimization of the mixed convection.

***Keywords*—**Entropy generation, mixed convection, conjugate heat transfer, numerical, nanofluid, wall waviness.

I. Introduction

NANOFLUID is a colloidal mixture of nano-sized particles of size up to 1-100 nm in a base fluid. These nano-sized particles are named as nanoparticles and they have tremendous impact on transport properties and heat transfer performance. Nanofluid has higher rate of heat transfer capability compared to traditional low thermal conductive base fluid such as water, oil etc. For this reason nanofluid has a widespread application in many industries and engineering branches where heat transfer is a primary need to sharp device performance.

Over the years nanofluids have received attracted attention by several researchers for its wide range of applications, mainly in the industry like cooling nuclear system, improving the efficiency of thermal management system, energy storage system, improvement of lubricants etc. Choi [1], who suggested the name "nanofluid" in 1995, studied theoretically the thermal conductivity of nanofluid consisting copper nanophase materials and conclude that not only nanofluid exhibit high thermal conductivity compared to the conventional base fluid (oil, water, ethylene glycol etc.) but also reduces heat exchanger pumping power. Another study by Xuan and Li [2] also admits the fact that suspension of nanoparticles into base fluid produces an enhanced rate of heat transfer.

Heat transfer related problems in an enclosure are often in use in many engineering applications and biological applications, such as cell transport in arteries and veins, the cooling of electronic system, nuclear reactors, lubricating grooves, solar absorber etc. Both, the buoyancy-induced and lid-driven flows have importance in these applications [3], [4]. Tiwari and Das [5], Abu-Nada and Chamkha [6], Rahman [7] and Khorasanizadeh et al. [8] studied mixed convection of nanofluid in an enclosure to analyze the behaviour of nanofluids and concluded by positive remarks as they found that the average Nusselt number of nanofluid is larger than that of the base fluid under the same Richardson number.

A number of efforts are made to study conjugate heat transfer in an enclosure. Oztop et al. [9] investigated conjugate mixed convection in an enclosure with thick bottom wall. Chamkha and Ismael [10] studied conjugate heat transfer in a cavity filled with nanofluids by considering a triangular thick wall which is heated in a porous medium. According to theses researchers wall thickness have a great contribution in heat transfer. Some researchers also studied mixed convection flow in an enclosure by considering different shape or orientation of the enclosure. Nayek et al. [11] investigated mixed convection in an skewed enclosure filled with Cu-water nanofluid and concluded that skew angel has a great contribution on heat transfer and entropy generation. Al-Amiri et al. [12] investigated mixed convection in an enclosure with sinusoidal wavy bottom surface and found that the average Nusselt number increases with as both the amplitude of the wavy surface and Reynolds number increases.

In this article, a numerical study is made on the mixed convection of copper-water nanofluid inside an enclosure with thick wavy bottom wall. The aim of this study is to investigate the effect of nanoparticles over flow field and heat transfer at different lower wall configurations. In addition, the entropy generation factor also has been analyzed. Coordinate transformation procedure has been applied to transform the computation domain into a square domain so that finite volume method can be applied. SIMPLE algorithm has been used to solve the pressure-velocity coupling.

II. Governing Equations

A two-dimensional mixed convection of Cu-water nanofluid in an square enclosure with thick wavy bottom wall has been

S. Bhattacharyya is with the Department of Mathematics, Indian Institute of Technology Kharagpur, Kharagpur-721302 (corresponding author, e-mail: somnath@maths.iitkgp.ernet.in).

Sanjib Kr Pal is with the Department of Mathematics, Indian Institute of Technology Kharagpur, Kharagpur-721302 (e-mail: sanjibkumarpal1@gmail.com).

considered, as shown in fig.1. The upper wall of the enclosure is on and along the positive x-axis and the $y = -H$ is the tangent line to the lower wavy wall. The top wall is at temperature T_c and is allowed to moves with an uniform velocity U_0 inducing shear in the flow. Lower wall is at temperature T_h and $T_h > T_c$. Vertical walls are kept insulated. However, the solid portion of the wall is considered of a constant thickness, say h.

The single phase model has been adopted for the present study. It is assumed that the base fluid and the nanoparticles are in thermal equilibrium and the radiative heat transfer, viscous dissipation, chemical reaction between base fluid and nanoparticles are negligible. Many researchers, such as Malvandi and Ganji [13], discussed the justification of these assumptions. Under the above assumptions, the governing equations for mixed convection in an wavy wall cavity with Boussinesq approximation in nondimensional form can be written as

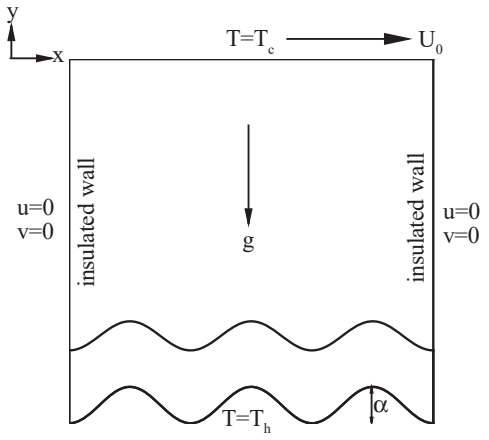

Fig. 1 Schematic diagram of physical space and coordinates

$$\frac{\partial u}{\partial x}+\frac{\partial v}{\partial y}=0 \tag{1}$$

$$\frac{\partial u}{\partial t}+u\frac{\partial u}{\partial x}+v\frac{\partial u}{\partial y}=-\frac{\partial p}{\partial x}+\frac{1}{Re}\frac{\rho_f}{\rho_{nf}}\frac{1}{(1-\phi)^{2.5}}\left(\frac{\partial^2 u}{\partial x^2}+\frac{\partial^2 u}{\partial y^2}\right) \tag{2}$$

$$\frac{\partial v}{\partial t}+u\frac{\partial v}{\partial x}+v\frac{\partial v}{\partial y}=-\frac{\partial p}{\partial y}+\frac{1}{Re}\frac{\rho_f}{\rho_{nf}}\frac{1}{(1-\phi)^{2.5}}\left(\frac{\partial^2 v}{\partial x^2}+\frac{\partial^2 v}{\partial y^2}\right)+\frac{Gr}{Re^2}\frac{\rho_f}{\rho_{nf}}\left(1-\phi+\phi\frac{\rho_p\beta_p}{\rho_f\beta_f}\right)\theta \tag{3}$$

$$\frac{\partial \theta}{\partial t}+u\frac{\partial \theta}{\partial x}+v\frac{\partial \theta}{\partial y}=\frac{k_{nf}}{k_f}\frac{(\rho C_p)_f}{(\rho C_p)_{nf}}\frac{1}{RePr}\left(\frac{\partial^2 \theta}{\partial x^2}+\frac{\partial^2 \theta}{\partial y^2}\right) \tag{4}$$

The dimensionless variables are defined by $(x,y)=\frac{(x^*,y^*)}{H}$, $t = t^*U_0/H$, $\alpha = \frac{h^*}{H}$, $\theta = \frac{T-T_c}{T_h-T_c}$, $(u,v) = \frac{(u^*,v^*)}{U_0}$, $p = \frac{p^*}{\rho_{nf}U_0^2}$, $g(x) = \frac{g^*(\frac{x^*}{H})}{H}$. The dimensionless parameters are Reynolds number $Re = \frac{\rho_f U_0 L}{\mu_f}$, Prandtl number $Pr = \frac{\nu_f}{\alpha_f}$.

The effective density of nanofluid is given by $\rho_{nf} = (1-\phi)\rho_f + \phi\rho_p$. Effective heat capacitance of nanofluid is given by $(\rho c_p)_{nf} = (1-\phi)(\rho c_p)_f + \phi(\rho c_p)_p$ [2]. The thermal diffusivity of nanofluid is expressed as $\alpha_{nf} = \frac{k_{nf}}{(\rho C_p)_{nf}}$ [14]. There exists several modified models for the dynamic viscosity of nanofluids but Brinkman model still gives reasonable result. So Brinkman model [15] has been adopted for effective viscosity of nanofluid, μ_{nf} and is given by $\mu_{nf} = \frac{\mu_f}{(1-\phi)^{2.5}}$, where ϕ is the nanoparticle volume fraction. The Maxwell−Garnetts model has been considered to determine the effective thermal conductivity of the nanofluid and is given by $\frac{k_{nf}}{k_f} = \frac{k_p+2k_f-2\phi(k_f-k_p)}{k_p+2k_f+\phi(k_f-k_p)}$. The thermo-physical properties for water and copper, at room temperature, used in this study, has been given in Table I.

TABLE I
THERMOPHYSICAL PROPERTIES OF WATER AND COPPER

Parameter	Water	Copper
$c_p(J/kgK)$	4179	383
$\rho(kg/m^3)$	997.1	8954
$k(W/mK)$	0.6	400
$\beta(K^{-1})$	2.1×10^{-4}	1.67×10^{-5}

The boundary conditions are as follows:
$u = 1,\ v = 0,\ T = 0$ at the top wall
$u = 0,\ v = 0,\ T = 1$ at the lower wall
$u = 0,\ v = 0,\ \frac{\partial T}{\partial x} = 0$ at the right wall
$u = 0,\ v = 0,\ \frac{\partial T}{\partial x} = 0$ at the left wall
At the solidfluid interface the equilibrium state is assumed to be verified. Hence the temperature and the heat flux must be continuous a5t the interface.

$\theta_w = \theta_{nf}$ and $k_w\frac{\partial \theta_w}{\partial n} = k_{nf}\frac{\partial \theta_{nf}}{\partial n}$, or, $\frac{\partial \theta_w}{\partial n} = K_r\frac{\partial \theta_{nf}}{\partial n}$, where n is the normal vector on the wavy interface and $K_r = \frac{k_w}{k_{nf}}$ is the thermal conductivity ratio and can be written as, $K_r = \frac{k_p+2k_f+\phi(k_f-k_p)}{k_p+2k_f-2\phi(k_f-k_p)}\frac{k_w}{k_f}$. For $\phi = 0.0$ K_r is denoted as $K_{r0} = K_r\mid_{\phi=0.0} = \frac{k_w}{k_f}$.

A co-ordinate transformation is introduced as

$$\xi = x, \eta = \frac{y}{g(x)} \tag{5}$$

where $g(x) = 1-\alpha[1+cos(2\pi x)]$ and $-g(x)$ is the shape of the rib mounted on the wall $y = -1$. Under this transformation the governing equations .(1)-(4) reduce to

$$\frac{\partial u}{\partial \xi}-\left(\frac{\eta}{g(\xi)}\right)\left(\frac{dg}{d\xi}\right)\frac{\partial u}{\partial \eta}+\frac{1}{g(\xi)}\frac{\partial v}{\partial \eta}=0 \tag{6}$$

$$\frac{\partial u}{\partial t}+\frac{\partial (u^2)}{\partial \xi}-\left(\frac{\eta}{g(\xi)}\right)\left(\frac{dg}{d\xi}\right)\frac{\partial (u^2)}{\partial \eta}+\frac{1}{f(\xi)}\frac{\partial (uv)}{\partial \eta}=$$
$$-\frac{\partial p}{\partial \xi}+\left(\frac{\eta}{g(\xi)}\right)\left(\frac{dg}{d\xi}\right)\frac{\partial p}{\partial \eta}+\frac{1}{Re}\frac{\rho_f}{\rho_{nf}}\frac{1}{(1-\phi)^{2.5}}$$
$$\times[\frac{\partial^2 u}{\partial \xi^2}+\left(\frac{\eta}{g(\xi)}\right)^2\left(\frac{dg}{d\xi}\right)\frac{\partial^2 u}{\partial \eta^2}-\left(\frac{2\eta}{g(\xi)}\right)\left(\frac{dg}{d\xi}\right)\frac{\partial^2 u}{\partial \xi\partial \eta}+$$

$$\left\{\frac{2\eta}{g^2(\xi)}\left(\frac{dg}{d\xi}\right)^2-\left(\frac{\eta}{g(\xi)}\right)\left(\frac{d^2g}{d\xi^2}\right)\right\}\frac{\partial u}{\partial\eta}] \quad (7)$$

$$\frac{\partial v}{\partial t}+\frac{\partial(uv)}{\partial\xi}-\left(\frac{\eta}{g(\xi)}\right)\left(\frac{dg}{d\xi}\right)\frac{\partial(uv)}{\partial\eta}+\frac{1}{g(\xi)}\frac{\partial(v^2)}{\partial\eta}=$$
$$-\frac{1}{g(\xi)}\frac{\partial p}{\partial\eta}+\frac{1}{Re}\frac{\rho_f}{\rho_{nf}}\frac{1}{(1-\phi)^{2.5}}$$
$$\times[\frac{\partial^2 v}{\partial\xi^2}+\left(\frac{\eta}{g(\xi)}\right)^2\left(\frac{dg}{d\xi}\right)\frac{\partial^2 v}{\partial\eta^2}-\left(\frac{2\eta}{g(\xi)}\right)\left(\frac{dg}{d\xi}\right)\frac{\partial^2 v}{\partial\xi\partial\eta}+$$
$$\left\{\frac{2\eta}{g^2(\xi)}\left(\frac{dg}{d\xi}\right)^2-\left(\frac{\eta}{g(\xi)}\right)\left(\frac{d^2g}{d\xi^2}\right)\right\}\frac{\partial v}{\partial\eta}] \quad (8)$$

$$\frac{\partial\theta}{\partial t}+\frac{\partial(\theta u)}{\partial\xi}-\left(\frac{\eta}{g(\xi)}\right)\left(\frac{df}{d\xi}\right)\frac{\partial(\theta u)}{\partial\eta}+\frac{1}{f(\xi)}\frac{\partial(\theta v)}{\partial\eta}=$$
$$\frac{k_{nf}}{k_f}\frac{(\rho C_p)_f}{(\rho C_p)_{nf}}\frac{1}{RePr}$$
$$\times[\frac{\partial^2\theta}{\partial\xi^2}+\left(\frac{\eta}{g(\xi)}\right)^2\left(\frac{dg}{d\xi}\right)\frac{\partial^2\theta}{\partial\eta^2}-\left(\frac{2\eta}{g(\xi)}\right)\left(\frac{dg}{d\xi}\right)\frac{\partial^2\theta}{\partial\xi\partial\eta}+$$
$$\left\{\frac{2\eta}{g^2(\xi)}\left(\frac{dg}{d\xi}\right)^2-\left(\frac{\eta}{g(\xi)}\right)\left(\frac{d^2g}{d\xi^2}\right)\right\}\frac{\partial\theta}{\partial\eta}] \quad (9)$$

A. Nusselt Number

The local Nusselt number along the interface within the nanofluid-saturated porous medium side can be written as:

The local Nusselt number (Nu) along the interface is defined as
$Nu=-\left(\frac{k_{nf}}{k_f}\right)\frac{\partial\theta}{\partial n}$

By integrating the local Nusselt number along the heated surface we have the average Nusselt number as
$Nu_{av}=\frac{1}{d}\int_0^d(Nu)ds$
where ds is elementary surface of the wall and d is the length of the wall.

B. Entropy Generation

The entropy generation for the thermodynamic optimization of the system has been analyzed based on the local thermodynamic equilibrium of linear transport theory [16]. The local entropy generation rate is produced in cavity is due to heat flow and viscous dissipation respectively. The local entropy generation, $S_{gen}=S_h+S_f$, for the nanofluid can be written in the nondimensional form [11], [16], [17] as

$$S_{gen}=(\frac{k_{nf}}{k_f})\left[\left(\frac{\partial\theta}{\partial\xi}-\frac{\eta}{g(\xi)}g'(\xi)\frac{\partial\theta}{\partial\eta}\right)^2+\left(\frac{1}{g(\xi)}\frac{\partial\theta}{\partial\eta}\right)^2\right]$$
$$+\chi\frac{\mu_{nf}}{\mu_f}[2\left\{\left(\frac{\partial u}{\partial\xi}-\frac{\eta}{g(\xi)}g'(\xi)\frac{\partial u}{\partial\eta}\right)^2+\left(\frac{1}{g(\xi)}\frac{\partial v}{\partial\eta}\right)^2\right\}$$
$$+\left\{\left(\frac{1}{g(\xi)}\frac{\partial u}{\partial\eta}\right)+\left(\frac{\partial v}{\partial\xi}-\frac{\eta}{g(\xi)}g'(\xi)\frac{\partial v}{\partial\eta}\right)\right\}^2] \quad (10)$$

where χ is the irreversibility factor and is defined as $\chi=\frac{\mu_f T_0 U_0^2}{k_f(T_h-T_c)}$. The term S_h is the local entropy generation due to heat transfer irreversibility and S_f is the local entropy generation due to fluid friction irreversibility. The entropy generation number is obtained by integrating S_{gen} over the whole computational domain V divided by the total volume of the domain i.e.,

$S_{tot}=\frac{1}{V}\int S_{gen}dV$

To explain the contribution of heat transfer irreversibility (S_h) and the fluid friction irreversibility (S_f) on S_{gen}, Bejan number is obtained as $Be=S_h/S_{gen}$. The average Bejan number is defined as $Be_{av}=\frac{1}{V}\int BedV$. It may be noted that $Be_{av}<0.5$ implies the dominance of fluid friction irreversibility while $Be_{av}>0.5$ implies the dominance of heat transfer irreversibility [11].

III. Numerical Methods

The set of transformed non-linear governing equations (7)-(9) were discretized and then solved using the finite volume method in its non-dimensional form on a staggered grid arrangement [18]. The computation domain was divided into control volumes and over each control volume the governing equations were integrated. The control volumes are different for each computing variables. In the staggered grid system, the velocity components are evaluated at the midpoint of the cell sides to which they are normal while the pressure and all the scalar quantities are stored at each cell center. The convective terms in the momentum and energy equations were discretized using QUICK (Quadratic Upwind Interpolation for Convective Kinematics) scheme [19] and second order central difference scheme was employed for the diffusion terms. SIMPLE (Fletcher [18]) algorithm was introduced to the velocity-pressure coupling.

At every time step the discretized equations were solved using block elimination method in a coupled manner. At each iteration level the pressure field was corrected and updated using the SIMPLE algorithm from a initial guess pressure. For any set of input parameters, the solution was considered converged if $max_{ij}\mid\Phi_{ij}^{k+1}-\Phi_{ij}^{k}\mid\leq 10^{-6}$ where subscripts i, j denote the cell index and superscripts k denotes the iteration index and Φ is the variable to compute.

A series of grid independency test was performed ranging from 41×41 to 81×81 which suggested that the grid independency can be archived using 51×51 grid system. The grid system considered here is uniform all over the computation domain. Fig.3(b). the local Nusselt number along the solid-liquid interface at Re=100 with $\omega=3$, $Ri=1.0$, $K_{r0}=1$ and $\phi=0.1$ and admits the optimality of 51×51 grid system. However, finer grids are used for higher Reynolds number.

The numerical procedure was validated by performing mixed convection flow with lid-driven in a cavity filled with nanofluid and the local Nusselt number along the hot wall was

compared with the calculation of Abu-Nada and Chamkha [6] and is given in Fig. 3 (a). for inclination angle 0° at $Ri = 1$, $Re = 10$ and $\phi = 0.1$. The present result shows very good agreement with the result due to Abu-nada and Chamkha [6]. For further more validation, we also compared the predicted temperature and stream function contours under steady state condition of the present work to that of Al-Amiri et al. [12] for $\alpha = 0.05$, $Pr = 0.71$, $Gr = 10^4$ and $Ri = 1$. An excellent agreement was archived as shown in Fig.3.

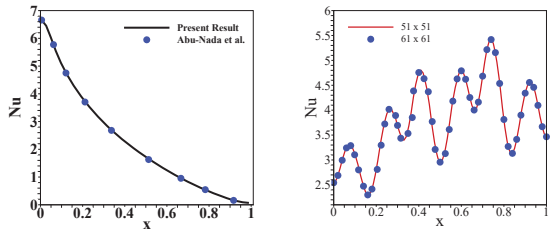

(a) (b)

Fig. 2 (a) Comparison of the streamlines and temperature contours between the present work [(c), (d)] and that of Al-Amiri et al. [12] [(a), (b)] for $\alpha = 0.05$, $Pr = 0.71$, $Gr = 10^4$ and $Ri = 1$, (b) Nusselt number Nu along the solid-liquid interface at Re=100 with $\omega = 3$, $Ri = 1.0$, $K_{r0} = 1$ and $\phi = 0.1$

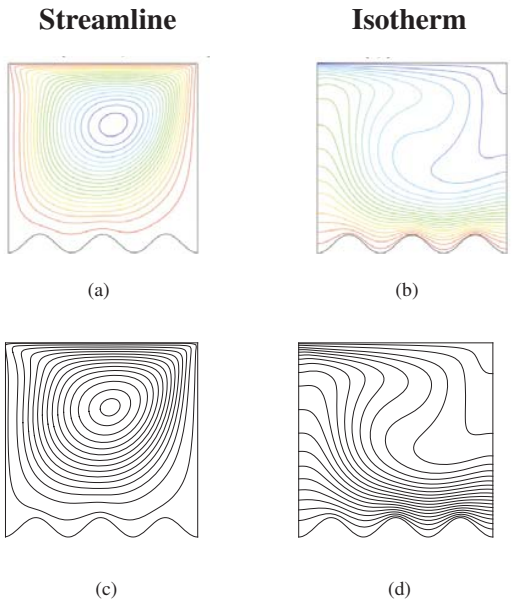

(a) (b)

(c) (d)

Fig. 3 Comparison of the streamlines and temperature contours between the present work [(c), (d)] and that of Al-Amiri et al. [12] [(a), (b)] for $\alpha = 0.05$, $Pr = 0.71$, $Gr = 10^4$ and $Ri = 1$

IV. Results and Discussion

We consider a conjugate mixed convection of Cu-water nanofluid in an enclosure with wavy solid portion of fixed thickness. Results presented here are very selective to preserve the brevity. The effect of five relevant parameters, namely, Richardson number ($0.1 \leq Ri \leq 5$), nanoparticle volume fraction ($0.0 \leq \phi \leq 0.2$), wave number ($0 \leq \omega \leq 3$), amplitude ($0 \leq \alpha \leq 0.1$) of the wavy solid and thermal conductivity ratio $K_{r0} = k_w/k_f$(23.8 stainless steelewater, 1.0 brickworkewater, 0.44 epoxyewater), have been discussed here. Flow and thermal fields are analyzed by the streamlines and isotherms. The Richardson number (Ri) has been varied keeping the Reynolds number (Re) fixed such that Grashof number (Gr) is varied between $10^3 \leq Gr \leq 5 \times 10^4$. The heat transfer enhancement is demonstrated by presenting the percentage difference of average Nusselt number for nanofluid from the corresponding pure fluid case with flat solid portion. To investigate the energy efficiency of the system, the total entropy (S_{tot}) and Bejan number (Be) have been studied.

Fig. 4 shows the effect of Richardson number (Ri) of Cu-water nanofluid streamline for different K_{r0} (=0.44, 1.0, 23.8) for three wave number (ω) at $\alpha = 0.1$. In every figure the effect of nanofluid volume fraction (ϕ) has been represented by solid lines ($\phi = 0.0$) and dashed lines ($\phi = 0.2$) respectively. The Richardson number provides an effective measurement of the natural convection forces over the mechanically lid-driven force convection effect. It can be seen from Fig. 4 that for $Ri = 0.1$, the fluid behaves like the classical lid-driven cavity problem where hot fluid rises from the lower heated thick wall and cooled by the moving cold lid. This gives a single circulation cell in the cavity, rotation in clockwise direction. This single circulation cell is also referred as primary vortex, which covers the whole cavity. The flow is characterised by another two eddies, a secondary eddy formed in the right lower corner of the cavity (referred to as the downstream secondary eddy) which is formed as a result of stagnation pressure and frictional losses and another secondary eddy, which is formed at the left side lower corner of the cavity (referred to as the upstream secondary eddy), formed due to the negative pressure gradient generated by the primary circulating fluid as it deflects upward over the upstream vertical wall. It can be seen that the upstream eddy vanishes as Ri increases and downstream eddy became larger. This is due to the fact that as Ri increases buoyancy is opposing the core flow which causes the boundary layer to detach from the wall making a larger eddy. For the nanofluid ($\phi = 0.2$), the size of the eddy is smaller. This is due to the fact that, as ϕ increases the contribution of the buoyancy term reduces. With the increase of Richardson number(Ri) the natural convection force also increases and hence the centre of the primary vortex moves towards the bottom wall.

Fig. 5 presents the isothermal contours for different K_{r0} (=0.44, 1.0, 23.8) for three wave number (ω) at $\alpha = 0.1$. Here conductivity ratio is considered as a governing parameter of the temperature distribution. When $K_{r0} = 0.44$, then the fluid inside the cavity became cold for the low conductivity of the solid wall. It behaves like an insulated wall and as a result the temperature field is distributed inside the solid wall. It makes the flow strength weaker. When $K_{r0} = 1.0$, then isotherms are in uniform manner and distributed uniformly near the wavy wall. When $K_{r0} = 23.8$, then wall conductivity become high and the flow behaves like the lid-driven cavity convection.

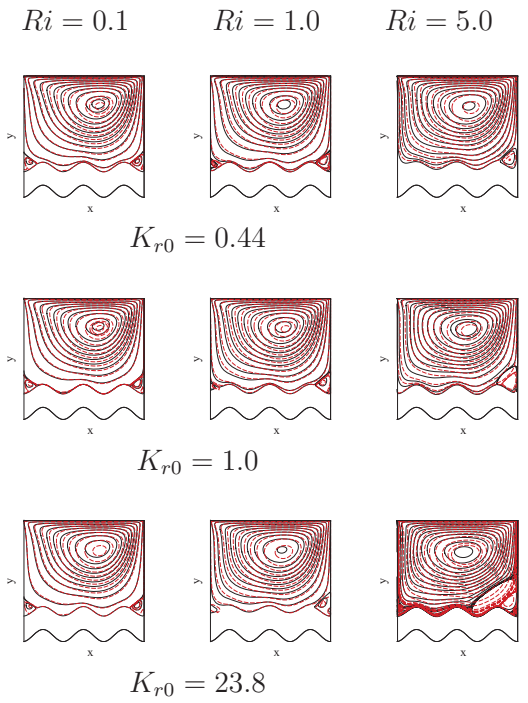

Fig. 4 Variation of streamlines for different K_{r0} and ϕ (dashed lines for $\phi = 0.0$ and solid lines for $\phi = 0.2$) at $Ri = 0.1, 1.0, 5.0$ (1st, 2nd and 3rd column respectively)

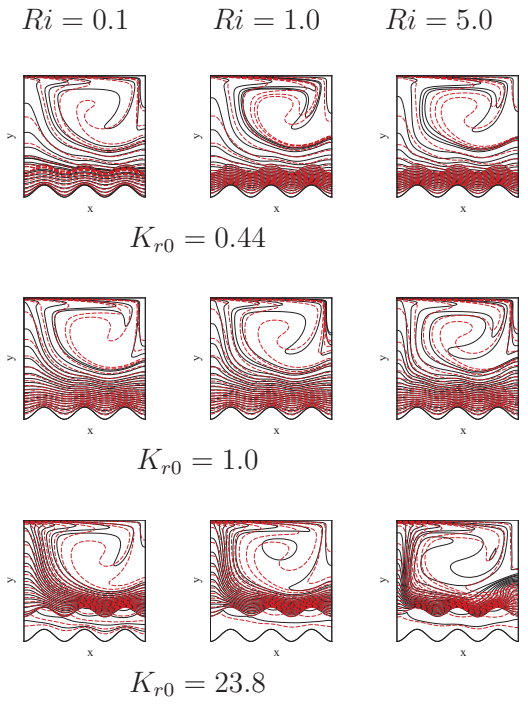

Fig. 5 Variation of isotherms for different K_{r0} and ϕ (dashed lines for $\phi = 0.0$ and solid lines for $\phi = 0.2$) at $Ri = 0.1, 1.0, 5.0$ (1st, 2nd and 3rd column respectively)

To investigate the In Fig. 6 the variation of κ is shown. It is clear from the figure that κ increases as wave number (ω) and amplitude (α) of the wavy wall increases. This is because of the fact that as wave number or amplitude increases, lower surface become larger. Hence a large quantity of cold fluid get in contact with the hot wall and absorb heat.

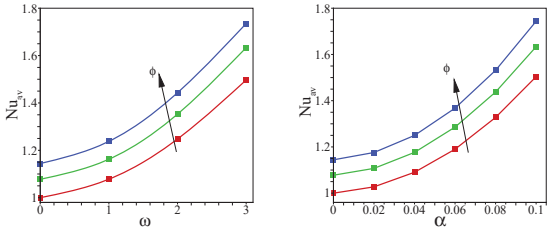

Fig. 6 Variation of Nusselt number increment ratio ($\kappa = Nu(\phi, \alpha = 0.1)/Nu(\phi = 0.0, \alpha = 0.0)$) with respect to (a) wave number (ω) and (b) amplitude of the wave (α) for $K_{r0} = 1$, $Ri = 1$

V. Conclusion

Conjugate mixed convection flow of Cu-water nanofluid in an enclosure has been studied. The flow and thermal fields are investigated using the contour plot of the steam line and isotherms. It is found that the waviness of the solid wall affects the heat transfer rate and increases with the wave number as well as the amplitude of the wavy wall. Flow fields are also affected by the waviness of the lower wall and the conductivity ratio of the wall and the water. It was also found that as Ri increases, the Nusselt number decreases. Similarly average entropy generation number also increases with the waviness of the solid wall. To make the presentation compact, results are not given here. Addition of nanofluid make the heat transfer rate higher.

References

[1] SUS Chol et al. Enhancing thermal conductivity of fluids with nanoparticles. ASME-Publications-Fed, 231:99-106, 1995.
[2] Yimin Xuan and Qiang Li. Investigation on convective heat transfer and flow features of nanofluids. Journal of Heat transfer, 125(1):151155, 2003.
[3] Benjamin Gebhart, Yogesh Jaluria, Roop L Mahajan, and Bahgat Sammakia. Buoyancy-induced flows and transport, 1988.
[4] PN Shankar and MD Deshpande. Fluid mechanics in the driven cavity. Annual Review of Fluid Mechanics, 32(1):93136, 2000.
[5] Raj Kamal Tiwari and Manab Kumar Das. Heat transfer augmentation in a two-sided lid-driven differentially heated square cavity utilizing nanofluids. International Journal of Heat and Mass Transfer, 50(9):20022018, 2007.
[6] Eiyad Abu-Nada and Ali J Chamkha. Mixed convection flow in a lid-driven inclined square enclosure filled with a nanofluid. European Journal of Mechanics-B/Fluids, 29(6):472482, 2010.
[7] Rahman, M. M., et al. Heat transfer enhancement of nanofluids in a lid-driven square enclosure. Numerical Heat Transfer, Part A: Applications 62.12 (2012): 973-991.
[8] Hossein Khorasanizadeh,Majid Nikfar, and Jafar Amani. Entropy generation of cuwater nanofluid mixed convection in a cavity. European Journal of Mechanics-B/Fluids, 37:143152, 2013.
[9] Hakan F Oztop, Changzheng Sun, and Bo Yu. Conjugatemixed convection heat transfer in a lid-driven enclosure with thick bottom wall. International Communications in Heat and Mass Transfer, 35(6):779785, 2008.
[10] Ali J Chamkha and Muneer A Ismael. Conjugate heat transfer in a porous cavity filled with nanofluids and heated by a triangular thick wall. International Journal of Thermal Sciences, 67:135151, 2013.
[11] RK Nayak, S Bhattacharyya, and I Pop. Numerical study on mixed convection and entropy generation of cuwater nanofluid in a differentially heated skewed enclosure. International Journal of Heat and Mass Transfer, 85:620634, 2015.

[12] Abdalla Al-Amiri, Khalil Khanafer, Joseph Bull, and Ioan Pop. Effect of sinusoidal wavy bottom surface on mixed convection heat transfer in a lid-driven cavity. International Journal of Heat and Mass Transfer, 50(9):17711780, 2007.
[13] Malvandi, A., and D. D. Ganji. Brownian motion and thermophoresis effects on slip flow of alumina/water nanofluid inside a circular microchannel in the presence of a magnetic field. International Journal of Thermal Sciences 84 (2014): 196-206.
[14] Ali J Chamkha and Eiyad Abu-Nada. Mixed convection flow in single-and double-lid driven square cavities filled with wateral 2 o 3 nanofluid: effect of viscosity models. European Journal of Mechanics-B/Fluids, 36:8296, 2012.
[15] HC Brinkman. The viscosity of concentrated suspensions and solutions. The Journal of Chemical Physics, 20(4):571571, 1952.
[16] Adrian Bejan. A study of entropy generation in fundamental convective heat transfer. ASME J. Heat Transfer, 101(4):718725, 1979.
[17] Adrian Bejan and J Kestin. Entropy generation through heat and fluid flow. Journal of Applied Mechanics, 50:475, 1983.
[18] Clive Fletcher. Computational techniques for fluid dynamics 2: Specific techniques for different flow categories. Springer Science & Business Media, 2012.
[19] T Hayase, JAC Humphrey, and R Greif. A consistently formulated quick scheme for fast and stable convergence using finite-volume iterative calculation procedures. Journal of Computational Physics, 98(1):108118, 1992.